PITH ESTIMATION ON ROUGH LOG END IMAGES USING LOCAL FOURIER SPECTRUM ANALYSIS

Rudolf Schraml and Andreas Uhl
Department of Computer Sciences, University of Salzburg
J.-Haringerstr. 2, 5020 Salzburg, Austria
{rschraml,uhl}@cosy.sbg.ac.at

ABSTRACT
The location of the pith is an important feature of cross sections from tree logs. Images of log ends can be taken at little cost and at almost every stage in the log processing chain. Analysing images of rough log ends automatically requires robust pith estimation. This work evaluates two pith estimation algorithms using four different local Fourier Spectrum analysis methods. Proving that size, selection and amount of annual ring sections have an impact on both algorithms, this work contributes to existing literature. In comparing experiments for pith estimation for digital images of rough log ends and computer tomography (ct) cross section images, this paper highlights the difficulties for pith estimation on rough log end images. Finally, our results show that peak analysis and principal component analysis for local Fourier Spectrum analysis achieve the best accuracy and timing performance for pith estimation on rough log end images.

KEY WORDS
Cross Section Analysis, Rough Log Ends, Pith Estimation, Fourier Spectrum Analysis, Image and Pattern Analysis

1 Introduction

Anatomically the pith is the growth centre of a tree stem. At the cross section of the tree stem the pith is the innermost point surrounded by annual rings. Annual rings and the pith are the only features that are always present. Thus, the pith is a unique point on a cross section. In determining the wood quality the pith position has two main functions: First, a pith located far away from the geometric center is an indicator for the presence of other wood properties like compression or reaction wood. Second, it represents a unique reference point for further analysis like annual ring counting or annual ring width measurement. Pith estimation is fundamental for cross section analysis.

Currently, cross section analysis of log ends are predominantly performed manually by visually inspecting logs. However, images of log ends can be taken with digital cameras at almost every stage in the log processing chain at little expenses. Automated image analysis applications can be established at the forest site and in the sawmill environment. Future approaches to analyse log end images can automate existing processes in the log processing chain, define new standards for measuring and grading logs, and can exploit novel applications, for example, to guaranty traceability of wood logs.

Previous approaches for analysing cross section images mostly rely on images from polished/sanded cross sections or ct-images. Ct-images are free of distortions caused by sawing or dust and the annual ring borders are slightly emphasized. Pith estimation approaches treating ct-images are presented in [1], [2], [3], [4]. All these approaches rely on annual ring analysis. Due to the distortions annual ring analysis approaches are not applicable to images of rough log ends.

Local orientation estimation approaches for pith estimation are shown in [5], [6] and [7]. The former two use local Fourier Spectrum analysis for pith estimation on rough log end boards and on well prepared cross section discs, respectively. The authors use the peak of the local Fourier spectrum as local orientation estimate of an annual ring section. Pith estimation approaches rely on the assumption that annual rings are concentric circles. Consequently, local orientation estimates point towards the pith. With intersection of the local orientations the pith position is determined. The experiments of [5] indicate that pith estimation using local Fourier Spectrum analysis could also be applied on images from rough log ends. So far the only work focusing on the treatment of images of rough log ends was presented by [7] utilizing two local Fourier Spectrum analysis methods suggested in [8] and [9]. Both methods determine local orientations by convolution of filter kernels in the spatial domain. Results of [7] show that the second method (Laplacian pyramids and linear symmetry) is more robust to disturbances. Even though [7] provides first important insights into pith estimation of rough log ends, the authors of [7] noticed that the used image test set is not appropriate to draw conclusions about the performance of pith estimation for rough log ends of a sawmill yard.

This work contributes to pith estimation by treating images from rough log ends of a sawmill yard. For this purpose the Peak Analysis Method ([5] and [6]) and further three Fourier Spectrum Analysis methods are used to compute local orientations of small sections from cross section images, denoted as annual ring sections. Contrary to [7] it is shown that local orientation estimation in the Fourier domain is applicable for annual ring sections from rough log ends. For estimating the pith position two different al-

gorithms for selecting annual ring sections and intersecting the gathered local orientations are assessed. One of these methods is based on the pith estimation algorithm presented in [6]. To the author's knowledge, no study so far has focused on the influence of the size and the selection of annual ring sections on the pith estimation accuracy and timing. Thus, this work additionally contributes to existing literature by showing that the size, the amount and selection of annual ring sections influence the accuracy and timing of the proposed methods for pith estimation.

The empirical study compares two different sets of cross section images. One image set consists of 109 images of rough spruce log ends from a sawmill yard. The other set is equal to the ct-image set used in the experiments of [4]. The results of the experiments of the ct-image set are compared to the results for pith estimation using annual ring analysis methods presented in [4]. The results of the proposed methods on the rough log end images are compared to those from [7].

Section 2 introduces the basics of local orientation estimation (subsection 2.1) and presents considerations about Fourier Spectra of annual ring sections (subsection 2.2). Subsequently, three Fourier spectrum analysis methods for local orientation estimation of annual ring sections are introduced (subsection 2.3). Two pith estimation algorithms for selecting annual ring sections and computing a pith estimate are presented in Section 3. Finally Section 4 describes and assesses the experiments on the two image sets.

2 Local Fourier Spectra Analysis of Annual Ring Blocks

All pith estimation approaches using annual ring analysis or local orientation estimation methods rely on the assumption that annual rings are concentric circles the center point of which is the pith position. Annual ring analysis focuses on finding and identifying annual rings. The detected annual rings or arcs are then used to compute orthogonal vectors pointing towards the pith or to compute annual ring/ arc centre points representing votes for the pith position. Regardless of using gradient operators, edge detectors or other methods to extract annual rings or arcs, it becomes impossible to extract valid data with increasing disturbances (see Section 2.2). Local orientation estimation methods show higher reliability in case of disturbances.

2.1 Local Orientation Estimation

Local orientation estimation is a widely used technique in image processing systems and especially in texture analysis. In [10] and [11] the terms "linear symmetry" and "simple neighbourhood" are introduced, respectively. These terms are based on images where the grey values are equal along lines and only change in one direction. Such images are called simple images. The direction in which the grey values vary is defined as the image orientation, denoted as a unit vector $\hat{n}$. A simple neighbourhood can be represented by a 1-dimensional function $f(x, y) = g(x) = g(x^T \hat{n})$ where $x^T \hat{n}$ denotes the scalar product [12]. Images that are not simple can be divided into image sections, which (approximately) fulfill the property of simple images. Image orientations of such simple image sections are referred to as "local orientation". The Fourier Spectrum of a simple image is represented by a single line that is equally oriented as the simple image. If the simple image can be described as a sinusoidal function it is represented by two points in the Fourier spectrum. The more the simple image deviates from being simple the more the Fourier Spectrum spreads.

2.2 Fourier Spectra of Annual Ring Sections

The energy distribution of annual ring sections in the Fourier Spectrum is influenced by the capturing device (ct-scanner, digital or infra-red camera, ...), the wood species (different wood species show different annual ring structures), wood properties visible at the cross section (e.g. knots), the wood surface (sanded or rough - chainsaw or circular saw), and several other disturbances (light conditions, soiling and dirt, cracks, ...).

Annual ring sections of ct-cross section images are nearly free from distortions and have similar properties as images from sanded/ polished log ends. Compared to images from rough log ends they show less cracks and no cutting distortions (compare the annual ring sections in Fig. 2 and Fig. 3).

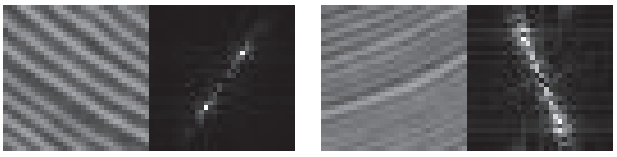

(a) consistent ring width (b) varying ring width

Figure 1: Annual ring sections from a ct-cross section image and their Fourier Spectra

Fig. 1 shows two annual ring sections from a ct-cross section image. The annual rings in Fig. 1(a) are consistent in width and are slightly curved. As a result the Fourier spectrum is concentrated around two points that reflect the main annual ring width and the annual ring orientation. In Fig. 1(b) the annual ring widths vary more strongly and the Fourier spectrum spreads from a point to a straight line.

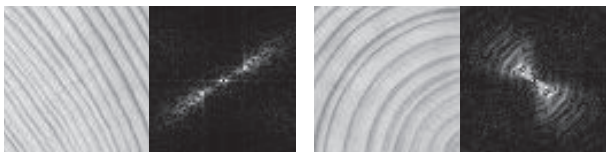

(a) section with low curvature (b) section close to the pith with high curvature

Figure 2: Annual ring sections from a sanded cross section and their Fourier Spectra

The annual ring sections in Fig. 2 are from a sanded log end face, captured under perfect light conditions. Apart from

the inverted colour (late wood is bright and early wood is dark) these annual ring sections are similar to those from ct-cross section images. Fig. 2(a) and Fig. 2(b) demonstrate the influence of the annual ring curvature on the Fourier Spectrum. The stronger the curvature, the more the line spreads and forms two circle sectors. The annual ring sections in Fig. 3 are from a rough log end image. It is obvious that the noise increases in the spatial domain as well as in the Fourier domain. While in Fig. 3(a) the dominant annual ring orientation is clearly visible, in Fig. 3(b) two different orientations are present. This typically occurs when the cutting pattern, cracks, knots or light shadows disturb the annual ring section. Commonly, many annual ring sections from a rough log end image are disturbed in such a way, so that no annual ring orientation can be determined.

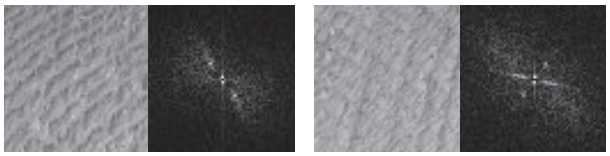

(a) slightly disturbed due to cutting (b) strongly disturbed due to cutting

Figure 3: Annual ring sections from a rough log end image and their Fourier Spectra

Subsequently, different approaches for local annual ring orientation estimation using Fourier Spectrum analysis are presented. All presented methods utilize the Fourier Spectrum of a given annual ring section as input. As results, all methods deliver an estimate of the orientation and if possible a certainty value of the estimate. For this purpose the size of the annual ring section in conjunction with the image resolution has to be chosen carefully. Basically, a higher image resolution provides more detailed information about the cross section, but on the other hand it suffers from additional noise in the Fourier Spectra of the annual ring sections. The size of the annual ring section determines the amount of included annual rings. The bigger the annual ring section, the higher the probability of a stronger annual ring curvature and a variation in width. These observations also affect the performance of the following methods to some extent.

2.3 Fourier Spectrum Analysis Methods

In this subsection the Peak Analysis method (c.f. [5] and [6]) and additionally three methods for local orientation estimation using Fourier Spectrum analysis are described. First, two approaches for Fourier Spectrum preprocessing of annual ring sections are described.

2.3.1 Fourier Spectrum Preprocessing

Two circumstances require a filtering of the Fourier Spectrum. First, it can be expected that the annual ring texture of an annual ring section is assigned to a certain bandpass in the Fourier Spectrum. Consequently, a bandpass filter filtering low and high frequencies is used to remove insignificant frequencies. Second, annual ring sections from images of rough log ends cause a very noisy Fourier Spectrum. A simple threshold is used to determine frequencies with a high magnitude. The threshold is calculated by determining two peaks of the Fourier Spectrum. If the ratio between them exceeds a certain value (e.g. 0.6) the threshold is set to T = max. peak $\cdot \lambda$, where λ is chosen in a range between 0.6 - 0.9. Otherwise it is assumed that the annual ring pattern is represented by the max. peak and just the maximum peak is further processed.

2.3.2 Peak Analysis - PA

PA is a very simple technique to gather a local orientation estimate. Linear symmetry assumes that the Fourier Spectrum of a simple image is aligned along a straight line. Disregarding the DC coefficient the maximum frequency should also lie on this line. Especially in the case of annual rings and appropriate section sizes, it can be assumed that the annual ring growth is approximately regular. The more uniform the local annual ring pattern is, the more the Fourier Spectrum converges to a single point. PA for pith estimation was introduced by [5] with the intention to count existing annual rings on rough log end boards from the two top end board edges into the direction of the pith. For this purpose, the presence of the pith on the board is not required. In this work the scope is to determine the exact pith position in images of rough log ends. For implementation a simple maximum search in one half-plane of the Fourier Spectrum has to be performed. The line through the Fourier Spectrum origin and the maximum coefficient of the preprocessed Fourier Spectrum is used as the local orientation estimate.

2.3.3 Least Squares Regression - LSR

Regarding the concept of linear symmetry, linear regression analysis is most qualified for orientation estimation. Linear regression methods enable the fitting of a line into a point cloud. Regardless if one or more explanatory variables describe one independent variable, simple or multivariate linear regression models are utilized. For linear symmetry analysis in the Fourier Spectrum the X and Y coordinates can be used alternatively as explanatory or independent variable.

The method of least squares regression is the best known method for fitting a regression line into a point cloud. Since LSR reduces the summed squared error (SSE) of the dependent variable it is necessary to determine the correlation coefficients of the X and Y values. If one axis shows a dominant correlation coefficient it is used as independent variable for the LSR. As certainty value the absolute coefficient of determination $|R^2|$ is computed and ranges between 0 and 1. For similar correlation coefficients (ratio > 0.8) LSR is computed with both axes as independent variables. Subsequently, the results are combined and the certainty value is set to 1. Finally the slope of the

regression line, representing the local orientation estimate and the certainty value, are received as results.

2.3.4 Weighted Least Squares Regression - WLSR

Due to the quadratic error weighting, LSR is very sensitive to outliers. A simple method to overcome the problem, that outliers from less significant frequencies influence the accuracy of LSR, is to utilize the magnitudes of the frequencies as weights $\beta = \frac{\sum(X_i \cdot Y_i \cdot W_i)}{\sum(X_i^2 \cdot W_i)}$. Due to the weighting - the frequencies with a high magnitude have more impact on linear regression than those with a low magnitude. As weight (W_i) for a given point in the Fourier Spectrum (X_i, Y_i) the square root of the related frequency magnitude (M_i) is used $W_i = \sqrt{M_i}$. Except from using weights, WLSR is performed in the same way as LSR to compute a local orientation estimate and the related certainty value.

2.3.5 Principal Component Analysis - PCA

PCA for texture orientation analysis using local Fourier Spectrum analysis was presented by [13]. In addition to determining a local orientation estimate PCA, can be used to make an assertion about the isotropy/ anisotropy of the analysed texture. Computationally PCA, is based on the Eigendecomposition of the covariance matrix for the XY coordinates. Eigendecomposition of the covariance matrix leads to two eigenvectors that represent the given points of the Fourier Spectrum. These two vectors are perpendicular to each other. The eigenvalues of the eigenvectors provide the information about the isotropy/ anisotropy. Anisotropy is used as a measure of the certainty of the orientation estimate. The more one eigenvector dominates, the more anisotropic is the distribution of the frequencies in the Fourier Spectrum. This means that an anisotropic distribution is an indicator of a simple image. For local orientation estimation the dominating eigenvector is utilized as the local orientation estimate. The ratio $\lambda = \frac{l_1 - l_2}{l_1}$ between the eigenvalue l_1 of the dominating eigenvector and the eigenvalue l_2 of the second eigenvector can be utilized as a certainty value

3 Pith Estimation Algorithms

This section describes two different algorithms for selecting annual ring sections/ image blocks and computing a pith estimate. The objective of both algorithms is to select image blocks and to compute local orientation estimates for each block. Finally, each algorithm uses the gathered local orientation estimates to perform an intersection step and to compute a pith estimate.

3.1 Block Area Selection - BAS

In [7], a rectangular area around the geometric image center is used to compute local orientation estimates for a subsequent intersection procedure. Knowledge about the cross section size and its location in the image is a precondition. After specifying an area it is subdivided into image blocks. Overlapping image blocks or a sliding window have the advantage that more annual ring orientations can be determined. The size of the blocks depends on the image resolution and on the cross section image type. Appropriate block sizes vary between 8x8 and 128x128 pixels. The experiments indicate that a lower resolution provides some advantages. High resolution images require a large blocksize and small structures and disturbances become visible.

In Fig. 4, subdivided rectangular and circular areas of two rough log end images are shown. The rectangle and circle dimensions were determined using the geometric image properties of the pre-cut images of rough log ends.

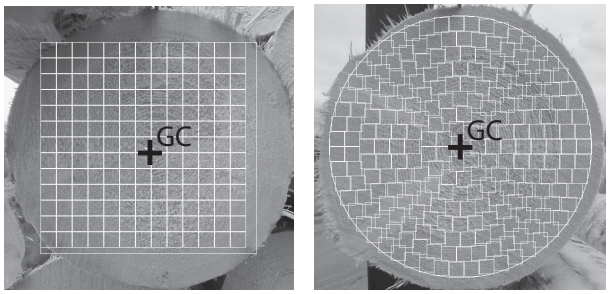

(a) Rectangular area and non-overlapping blocks (32x32 pixels) (b) Circular area and non-overlapping blocks (32x32 pixels)

Figure 4: Two cross section images from the rough log end image set (RLE-IS) with two different predefined areas for BAS

For all selected blocks, a local orientation estimate is computed using one of the Fourier Spectrum analysis methods. Expect for the PA method, a certainty value is additionally determined. Finally, local orientation estimates with a certainty value exceeding a certain threshold are further processed, (in the case of the PA method all local orientation estimates are further processed). Similar to [5] and [7] an accumulator array is used to sum up the intersections of all valid local orientation estimates. Finally, the accumulator array is filtered with a Gaussian smoothing kernel and the maximum accumulator value is assumed to hold the pith position. The Gaussian filter flattens local peaks and summarizes peak groups to a single peak. Fig. 5(a) shows an intersection image where a rectangular area and non-overlapping blocks with 32x32 pixels were used. It is clearly visible that the line intersections concentrate around the pith periphery.

3.2 Pointwise Block Selection - PBS

In [6], another technique that uses the geometric image center (GC) as initial reference point is presented. The principle of this technique is that first, two points around a reference point are chosen. Then, two local orientation estimates are calculated for the annual ring sections around these points. The intersection of these orientations is used as a new reference point. The procedure stops after a certain number of iterations or if the new reference point is

close to the old one. The concept of this technique is based on the assumption that annual rings close to the pith are more circular. Optimally, the pith estimate accuracy increases after performing several iterations.

For the experiments [6] used images from well prepared log end images. Preliminary experiments showed that pith estimation using only two local orientation estimates (in each iteration) becomes more inaccurate the more disturbed the cross section image. In the present work an extension of the suggested technique is introduced to overcome problems caused by inaccurate local orientation estimates. The GC is used as the initial reference point. In contrast to [6], the number of points can be chosen individually. These points are equally distributed on a circle described by a predefined radius around the reference point. Each point is used as a center point of an image block

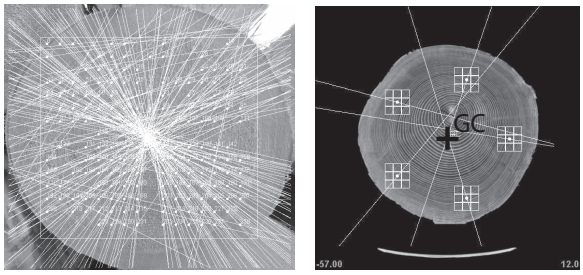

(a) BAS Intersection on a rough log end image

(b) PBS/ ct-cross section image where 5 points with a cluster size of 3x3 blocks were chosen

Figure 5: Intersection Images

cluster. A cluster consists of an arbitrary number of blocks. For each block of a cluster, the local orientations and certainty values are calculated. The information of all blocks of a cluster are then used to determine whether a valid cluster orientation estimate can be calculated. If not, a new point on a reduced radius, closer to the reference point is chosen and the cluster orientation estimation procedure repeats. After a certain number of unsuccessful iterations the procedure is cancelled and it is continued with the next initially chosen point. The cluster orientation estimation procedure is performed for all initially chosen points. At least two valid cluster orientation estimates are necessary to perform an intersection procedure. Finally, the barycentre of the intersections of all valid cluster orientations is chosen as the intermediate pith position. This one is utilized as new reference point and the whole procedure is repeated with a decreased radius. The algorithm terminates if the distance between the old and new pith position is under a certain limit or if a certain number of iterations were performed. In Fig. 5(b) a ct-cross section image is depicted where one iteration of the described algorithm has been performed. Five points in a radius of 120 pixels around the GC were chosen. For all clusters a valid cluster orientation estimate could be computed. Each cluster consists of 9 - 16x16 pixel blocks. The barycentre, which is assumed to hold the pith position, is not marked. PBS has the advantage that only a few blocks have to be analysed, keeping the computational effort low.

4 Experiments

The experiments provide information about the pith estimation performance of the two pith estimation algorithms (BAS, PBS) utilizing Fourier Spectrum analysis methods for local orientation estimation. The focus is to evaluate the performance and applicability of the particular Fourier Spectrum analysis methods for analysing annual ring sections from rough log end images. Results for a ct-cross section image set (CT-IS), using the same images as in [4], show how the proposed methods perform on less disturbed images. The accuracy of the proposed methods on the rough log end image set (RLE-IS) is compared to the results presented in [7].

The pith estimation performance is evaluated by computing several statistical values. The mean (Mean) describes the deviation from all epp (estimated pith positions) to the corresponding mpp (measured pith positions). StDev is the standard deviation from the Mean. R is defined as the span between the maximum and minimum pith estimation deviation. #Blocks (#B) gives the number of valid blocks that exceed the certainty threshold and are finally used for the intersection step. Finally, the computation time in milliseconds [ms] specifies the demand for the whole pith estimation process, except file IO.

Subsequently, for each of the two image sets the accuracy and the timing performance for pith estimation using the two pith estimation algorithms and different Fourier Spectrum analysis methods are presented. As a next step, the results are summarized and general conclusions about the accuracy and the timing performance of the particular configurations are drawn. All experiments were performed on an Intel Core i7-2620M processor with 2.7 GHZ and 8GB RAM, JRE 1.6.

Image Sets

Two different cross section image sets are used to evaluate the performance of the presented Fourier Spectrum analysis methods. One image set (CT-IS) was captured with a ct-scanner. It consists of 36 (512x512 pixels) cross section images taken from a single log. This image set was also used for the pith estimation experiments in [4]. The second image set (Rough Log End Image Set / RLE-IS) consists of 109 (1024x768 pixels) spruce log end images captured with a digital camera (Samsung WB2000). These images were taken on a sawmill yard in Austria without flash and at approximately the same distance from the log end surface to the camera. Consequently, one pixel corresponds to approximately 1.7 mm. The captured images represent log ends and their features found on a sawmill yard processing spruce logs. Log ends without any visible annual rings have been excluded. At the sorting station all log ends were cut by a circular saw. The ground truth (measured pith position - mpp) for both image sets was determined by visual inspection. Due to the approximately equal cross section size in all images of the CT-IS no localization of the cross section is necessary. The diameters of the log ends in the RLE-IS vary between 25 and 50 cm. For simplification the

images were pre-cut to the size of the log end sizes.

4.1 CT-IS Experiments

For pith estimation on the CT-IS the two pith estimation algorithms (BAS, PBS) are tested with each of the four Fourier spectrum analysis methods. For this purpose three configurations are selected and evaluated in detail. The first configuration (CT-BAS-C1) uses non-overlapping 16x16 pixels blocks and a rectangular BAS. The second configuration (CT-BAS-C2) first applies CT-BAS-C1. Based on the assumption that annual rings close to the pith are more circular, an 80x80 pixels rectangular area around the first pith estimate is defined. Local orientation estimates closer to the pith should point more precisely to the pith position. Subsequently, a second BAS with non-overlapping 8x8 pixel blocks is performed with the newly defined area. The second pith estimate is used as the final pith estimate. For both configurations the accumulator array is smoothed with a Gaussian filter with $\sigma = 1$, before the maximum value is determined.

The third configuration (CT-PBS-C3) uses the PBS algorithm. Five clusters with 16x16 pixel blocks are selected at each iteration. Each cluster consists of 4 blocks and at maximum 5 iterations are performed for estimating the final pith estimate. The radius for the first iteration was set to 100 pixel and decreases by a factor of 0.6 for each iteration. As termination criteria between the results of two iterations a value of 2 pixel is used.

The particular configurations and Fourier Spectrum analysis methods are tested with different certainty thresholds in a range between 0.3 and 0.9. For each configuration and Fourier Spectrum analysis method the most accurate result gathered with a particular certainty value is selected for the statistical analysis illustrated in Table 1. For PA no certainty value is computed and so #Blocks in the PA results using BAS gives the total number of selected blocks in the rectangular area. Comparing the results from CT-BAS-C1 and CT-BAS-C2, the accuracy of all methods in the latter configuration increases remarkably. On the other hand the timing performance decreases due to the higher amount of blocks. Although the certainty thresholds are very restrictive, a high amount of blocks (compared to the total amount of blocks in the PA results) are used for the intersection procedure. This shows that in ct-images only a few blocks are too disturbed to compute a local orientation estimate with a high certainty.

Config.	Method	C	Mean	StDev	#B	R	[ms]
CT-BAS-C1	PA	-	4.65	1.12	249	6	211
	LSR	0.9	4.86	1.3	234	7	196
	WLSR	0.9	4.78	1.25	243	7	202
	PCA	0.9	4.78	1.19	230	7	199
CT-BAS-C2	PA	-	3.08	1.68	346	7	303
	LSR	0.5	2.27	1.0	330	4	307
	WLSR	0.9	2.41	1.1	339	5	304
	PCA	0.7	2.46	1.35	335	6	303
CT-PBS-C3	PA	-	6.54	8.55	117	45	21
	LSR	0.9	2.16	1.75	118	8	22
	WLSR	0.9	1.86	1.3	114	5	21
	PCA	0.7	1.49	1.06	111	4	21

Table 1: CT-IS Pith Estimation - statistical analysis of three configurations. Mean, StDev and R are given as pixel values.

Surprisingly, the best results are reached with CT-PBS-C3 using the three introduced Fourier Spectrum analysis methods. Compared to the two other configurations this method is ten times faster and uses least blocks. The PA method shows a bad performance for CT-PBS-C3. This behaviour can be explained with the missing of a certainty value. Thus, wrong orientation estimates are not sorted out and affect the pith estimation accuracy. In Fig. 6 the results of the most accurate method for each configuration are depicted. In the experiments of [4] the best results were reached with the method that used sets of equal gradients and the circle equation: Mean - 2.8 pixels and Timing 16.64 seconds without preprocessing. Except the results using PA in CT-BAS-C2 and CT-PBS-C3 all methods outperform this mean value. Considering the timing performance it is shown that the proposed methods are very fast compared to the annual ring analysis methods evaluated in [4]. Additionally, no image preprocessing is required for the Fourier Spectrum analysis methods. The experiments on the CT-IS demonstrate that all proposed methods are well-suited for pith estimation on less disturbed cross section images.

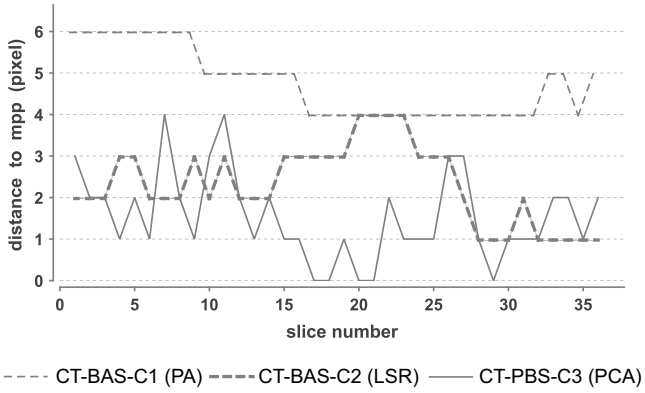

Figure 6: CT-IS — Best methods of each configuration

4.2 RLE-IS Experiments

As in the CT-IS experiments, seven configurations are selected and evaluated in detail. These configurations are divided into four groups (see Table 2). The first three groups present results for rectangular and circular BAS using non- and half-overlapping 16x16 pixels blocks. While in the first two groups it is tried to cover a large area from the log end face (see Fig. 4), the third group uses a smaller 300x300 pixels rectangular area around the GC. Equal to the CT-BAS-C2 configuration the third group uses the assumption that annual rings close to the pith are more circular. Compared to the CT-IS Experiments a larger Gaussian filter with $\sigma = 3$ was applied to the accumulator array of

the BAS configurations. Finally, the fourth group presents results for pith estimation using the PBS algorithm. For this purpose 20 clusters, each cluster consisting of four - 16x16 pixel blocks, are selected at each iteration. No more than six iterations are performed with a termination limit set to a value of 4 pixels. In Table 2 a statistical analysis for the most accurate configurations is presented. Because all configurations achieve at least one exact pith estimate - R also gives the most deviating pith estimate. For

Config		Method	C	Mean	StDev	#B	R	[ms]
Rectangular BAS-1	non overlapping	PA	-	5.56	4.43	710	25	1048
		LSR	0.9	6.45	5.08	643	27	1008
		WLSR	0.9	6.49	5.09	689	31	1032
		PCA	0.5	5.75	4.3	660	25	1036
	half overlapping	PA	-	3.49	2.53	2789	13	2453
		LSR	0.9	4.36	4.01	2528	24	2306
		WLSR	0.9	4.2	3.81	2709	25	2357
		PCA	0.9	4.03	3.23	1697	15	2003
Circular BAS	non overlapping	PA	-	6.57	4.55	798	22	1053
		LSR	0.9	6.0	4.7	720	27	960
		WLSR	0.9	6.43	5.56	481	34	858
		PCA	0.9	6.02	5.25	310	33	818
	half overlapping	PA	-	3.73	3.15	2118	20	1969
		LSR	0.9	4.43	4.39	1923	30	1888
		WLSR	0.5	4.19	4.25	2097	30	1962
		PCA	0.9	4.39	3.77	1296	25	1650
Rectangular BAS-2	non overlapping	PA	-	4.67	3.05	321	17	768
		LSR	0.9	5.91	5.1	295	33	761
		WLSR	0.5	6.46	6.7	319	45	771
		PCA	0.7	5.45	4.2	262	21	749
	half overlapping	PA	-	3.04	2.43	1284	13	1393
		LSR	0.9	3.38	3.37	1178	19	1355
		WLSR	0.3	3.01	2.49	1279	15	1396
		PCA	0.9	3.1	2.34	785	11	1193
PBS	20 - Cluster	PA	0.9	6.87	7.38	417	65	150
		LSR	0.7	8.19	9.1	390	50	178
		WLSR	0.7	8.37	9.53	402	48	184
		PCA	0.9	6.23	7.22	299	54	229

Table 2: RLE-IS Pith Estimation - statistical analysis of 9 configurations. Mean, StDev and R are given as mm values.

the configurations using BAS it can be summarized that configurations using PA and half-overlapping blocks entail very accurate estimates. The visual inspection of the pith estimates showed that non-overlapping blocks cause inaccuracies due to the large distances between the orientation estimates. For 16x16 pixels blocks half-overlapping blocks reduce this effect significantly (see Fig. 7). Additionally, it turned out that a higher amount of blocks, on the same area, almost always increases the accuracy and on the other hand it worsens the timing performance. For the circular BAS it was assumed that due to the optimal covering of the log end face the accuracy increases significantly. Results from Rectangular BAS-2, considering a smaller rectangular area around the GC, indicate that it is more essential to consider the area around the pith position in detail.

Overall configurations Rectangular BAS-2 using half-overlapping blocks reaches the best performance regarding the accuracy and timing performance for all methods. The best accuracy was reached with PCA (mean: 3.1 and StDev: 2.34) where all pith estimates are located within 11mm to the mpp (see Fig. 7).

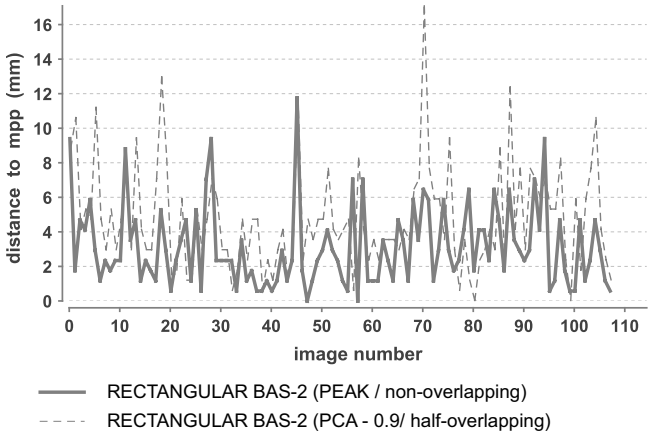

Figure 7: RLE-IS Pith Estimation accuracy - Rectangular BAS-2 with non-overlapping and half-overlapping blocks

Compared to the CT-IS Experiments the Fourier Spectrum threshold and the orientation certainty values have a major impact on the accuracy. Although the PA method assesses all blocks as valid, it is remarkable that the PA results are very accurate and robust regarding the StDev and R values. Because all blocks are valid - all blocks are used for the intersection procedure and thus slow down the pith estimation algorithm. Compared to the CT-IS experiments it can be recognised that higher certainty thresholds (C) reduce the amount of #Blocks to a higher degree. Since Fourier Spectrum preprocessing in the CT-IS and RLE-IS experiments was performed with the same parameters, the decreasing amount of #Blocks confirms that annual ring sections from rough log ends and their related preprocessed Fourier Spectra contain more disturbances. Thus, a huge amount of local orientation estimates have lower certainty values. In contrast to the PA method the introduced methods require that Fourier Spectrum thresholding filters out insignificant frequencies. Too low a threshold may have the affect that the introduced methods compute incorrect local orientation estimates and certainty values.

Comparing the PA and PCA results (Rectantgular BAS-2) it can be recognised that the PCA method assessed 500 blocks as not valid and is thus faster and additionally achieves a slightly better accuracy regarding the StDev and R values. It can be concluded that the PCA method provides reliable certainty values for all configurations using BAS and thus improves the timing performance neglecting disturbed blocks. LSR and WLSR also improve the timing performance, but they are almost always less robust regarding the StDev and R values.

Results from the fourth group show that the PBS algorithm is less suitable for rough log end images. Although the mean values are in a range between 6.23 and 8.37 pixels some unacceptable outliers are included. The best accuracy for PBS is reached with PCA (mean: 6.23 StDev: 7.22). Although the PCA method used fewest of all blocks

for determining the final pith estimate it was slower than the other methods. Similar to the BAS configurations the PCA methods assess a huge amount of blocks as not valid and thus more iterations to find valid clusters are required. As for the PBS results in the CT-IS experiments the PA method is very fast since no certainty values are available and thus valid clusters are found faster.

Finally, the accuracy is compared to the results presented in [7] using the Ultuna image set. This one consists of 20 log end images captured from 10 logs. Except for one pith estimate all deviations were smaller than 4 mm for the approach using Laplacian pyramids and linear symmetry [7]. Compared with the best configuration in Table 2 (Rectangular BAS-2 - PCA with half-overlapping blocks - mean: 3.1, stdev: 2.34) the accuracies are somewhat equivalent. Unfortunately in [7] no timing measurements are presented.

However, the experiments show that the proposed methods show an acceptable performance for spruce log end images of a sawmill yard. Results show that BAS and Fourier Spectrum analysis methods are well suited for pith estimation on rough log ends.

5 Conclusions

The experiments on the two different cross section image sets (CT-IS and RLE-IS) showed that local orientation estimation with Fourier Spectrum analysis methods are fast, robust, and very accurate in estimating the pith position. Results of the two pith estimation algorithms and the comparison of four Fourier Spectrum analysis methods highlighted the difficulties of pith estimation on images from rough log ends. The introduced PBS pith estimation algorithm achieves the best performance in the CT-IS experiments, but results show that the algorithm is inappropriate for pith estimation on images from rough log ends.

Although the PA method uses the least information of the Fourier Spectrum and provides no certainty value it reaches very accurate results for pith estimation using BAS. PCA shows a good reliability for determining valid orientation certainty values and improves the timing performance for BAS pith estimation significantly. Eventually, it was shown that it is more essential to consider sections close to the pith than to consider as much area as possible from the cross section.

Generally, it can be summarized that the block size, the distribution and amount of the blocks as well as Fourier Spectrum preprocessing are very important for pith estimation on images from rough log ends. Future research should develop more sophisticated block selection techniques. Especially for images from rough log ends a proper segmentation (using Fourier Spectrum Analysis) of the cross section could further increase the pith estimation accuracy.

References

[1] S. Bhandarkar, T. Faust, and M. Tang, "A system for detection of internal log defects by computer analysis of axial ct images," in *Procs. of the 3rd IEEE Workshop on Applications of Computer Vision*, Sarasota, USA, 1996, pp. 258–263.

[2] J.-P. Andreu and A. Rinnhofer, "Automatic detection of pith and annual rings on industrial computed tomography log images," in *Procs. of the 9th International Conference on Scanning Technology and Process Optimization for the Wood Industry*, Washington, USA, 2001, pp. 37–47.

[3] F. Longuetaud, J.-M. Leban, F. Mothe, E. Kerrien, and M.-O. Berger, "Automatic detection of pith on ct images of spruce logs," *Computers and Electronics in Agriculture*, vol. 44, no. 2, 2004, pp. 107–119.

[4] K. Entacher, S. Hegenbart, J. Kerschbaumer, C. Lenz, D. Planitzer, M. Seidel, A. Uhl, and R. Weiglmaier, "Pith detection on ct-cross-section images of logs: An experimental comparison," in *Procs. of the 3rd International Symposium on Communications, Control and Signal Processing*, St.Julians, MT, 2008, pp. 478–483.

[5] T. Hanning, R. Kickingereder, and D. Casasent, "Determining the average annual ring width on the front side of lumber," in *Procs. of SPIE: Optical Measurement Systems for Industrial Inspection*, W. Osten, M. Kujawinska, and K. Creath, Eds., vol. 5144, Munich, GER, 2003, pp. 707–716.

[6] P. Österberg, H. Ihalainen, and R. Ritala, "Method for analyzing and classifying wood quality through local 2d-spectrum of digital log end images," in *Procs. of International Conference on Advanced Optical Diagnostics in Fluids*, Tokyo, JP, 2004.

[7] K. Norell and G. Borgefors, "Estimation of pith position in untreated log ends in sawmill environments," *Computers and Electronics in Agriculture*, vol. 63, no. 2, 2008, pp. 155–167.

[8] H. Knutsson and G. H. Granlund, "Texture analysis using two-dimensional quadrature filters" in *IEEE Computer Society Workshop on Computer Architecture for Pattern Analysis and Image Database Management*, Pasadena, USA, 1983.

[9] J. Bigun, "Frequency and orientation sensitive texture measures using linear symmetry," *Signal Processing*, vol. 29, 1992, pp. 1–16.

[10] J. Bigun and G. H. Granlund, "Optimal orientation detection of linear symmetry," in *Procs. of the IEEE First International Conf. on Computer Vision*, London, GB, 1987, pp. 433–438.

[11] G. H. Granlund and H. Knutsson, *Signal Processing for Computer Vision*. (Dordrecht: Kluwer Academic Publishers, 1995).

[12] B. Jähne, *Digital Image Processing*, 5th ed. (Berlin Heidelberg: Springer, 2005).

[13] B. Josso, D. R. Burton, and M. J. Lalor, "Texture orientation and anisotropy calculation by fourier transform and principal component analysis," *Mechanical Systems and Signal Processing*, vol. 19, no. 5, 2005, pp. 1152–1161.